SELF-ASSEMBLY OF MONOLAYER-COATED SILVER NANOPARTICLES ON GOLD ELECTRODES. AN ELECTROCHEMICAL INVESTIGATION

Massimo MARCACCIO[1], Massimo MARGOTTI[2], Marco MONTALTI[3], Francesco PAOLUCCI[4,*], Luca PRODI[5] and Nelsi ZACCHERONI[6,*]

Dipartimento di Chimica "G. Ciamician", Università di Bologna, Via Selmi 2, 40126 Bologna, Italy; e-mail: [1] maxmar@ciam.unibo.it, [2] massimomargotti@ciam.unibo.it, [3] mmont@ciam.unibo.it,[4] paolucci@ciam.unibo.it, [5] lprodi@ciam.unibo.it, [6] nelsiz@ciam.unibo.it

Received May 27, 2003
Accepted July 9, 2003

This paper is dedicated to Professor Sergio Roffia, an esteemed scientist and a great teacher.

Redox behaviour of an array of dodecanethiol-coated silver nanoparticles, self-assembled on the gold electrode surface by dithiol linkers, is dominated in aqueous electrolytes by a reversible faradaic process that has been attributed to the anodic oxidation of silver nanoparticles. The nanoparticle array may be switched between the oxidised and reduced states repeatedly without any significant loss of electroactive material, thus showing a remarkable stability under electrochemical conditions. The mainly capacitive high-frequency electrical response of the nanoparticle array/electrolyte interface is characterised by a low value of capacitance, typical of a self assembled monolayer (SAM) of long-chain alkanethiols on gold; it has been associated with the compact organic layer interposed between the nanoparticles and the gold substrate. At lower frequencies, the interface displays a poorer electrical behaviour with both capacitive and resistive elements, which was associated with the more disordered organic layer located on the outer side of the film.

Keywords: Silver nanoparticles; Electrochemistry; Cyclic voltammetry; Electrochemical impedance spectroscopy; Self assembled monolayers.

The wide interest in the recent years in nanoscale engineering has been testified by the huge and permanently increasing amount of available literature on this topic, which describes many attempts to realise devices in the nanoscale range capable of performing useful functions[1,2], such as miniaturised sensing units[3,4] and data processing elements[5,6] for various applications[7]. Facing the problem from a chemical point of view, there is a need for systems extremely well characterised at the molecular level, since dealing with nanoscale materials means exploring properties derived from quantum-level phenomena and not (or not only) from macroscopic proper-

ties. In this context, nanoparticles are attracting much interest since their properties can be tuned on changing their dimensions[8] and/or the species linked on their surface, imparting them extremely varied chemical, electrical and optical characteristics[9–11]. In particular, self-assembly of metal nanoclusters on a variety of substrates, forming either 2D or 3D structures[12] and superstructures[13], has been widely investigated over a number of years[12–14]. Various strategies for the fabrication of such systems have been reported which generally exploit bifunctional ligands to accomplish either the interparticle linking and/or their anchoring onto the substrate surface[12–14]. Nanoparticles arrays of either metallic or semiconducting materials, organised into controlled architectures on relevant electronic substrates, have been, for instance, investigated for the fabrication of new generations of electronic devices and for sensor applications[14]. Electrochemistry has provided useful tools for the characterisation of such systems[12e,12h,12j,12k,13c,15,16], and, in particular, most of the electrochemical investigations on monolayer-protected nanoparticles have focused on the peculiar, size-dependent electrical properties of the nanoparticles/electrolyte interface[15]. Surface assemblies of gold or silver nanoparticles on gold or Al_2O_3 electrodes display in fact (sub)attofarad molecular capacitor characteristics[15], similar to those of solutions of non-anchored nanoparticles[16]. By contrast, other important aspects of the electrochemical behaviour of these systems, such as the stability of the organised assembly on electrochemical modifications of the nanoparticle surface, *e.g.*, the anodic growth of oxide films, have received relatively less attention[14].

We would like therefore to present here a detailed electrochemical study of monolayer-coated silver nanoparticles covalently linked to a gold electrode. Besides its implication in electronic devices, such system may also be potentially interesting, due to the reported biological activity of silver/silver oxide nanoparticles[17], for the realisation of antimicrobial coatings in biomedical devices. The strategy that we have followed for the construction of the nanoparticle array, takes advantage from the great affinity that gold and silver have for the thiol function. We have synthesised silver nanoparticles bearing dodecane-1,12-dithiol on the surface, one of the terminal SH function being linked to the silver surface and the other, to be linked to the gold electrode.

EXPERIMENTAL

Materials

Decane-10-thiol (**1**), all salts and solvents were obtained from Aldrich and used as supplied. Water of MilliQ grade was used.

Synthesis of Dodecane-1,12-dithiol (**2**)

1,12-Dibromododecane (6.0 mmol) and thiourea (7.8 mmol) were refluxed in water (15 ml) for 20 h. Next, 1.5 M sodium hydroxide (10 ml) was added and the reflux continued for another 6 h. A white precipitate appeared on cooling. It was filtered off after having set pH to 1.0 by adding a concentrated solution of sulfuric acid and copiously washed with water to afford 0.42 mmol of pure product. ^{1}H NMR (300 MHz, $CDCl_3$; δ, ppm): 2.5 (q, 4 H, C**H**$_2$SH), 1.6 (quintet, 4 H, C**H**$_2$CH$_2$SH), 1.3 (m, 16 H, (C**H**$_2$)$_8$CH$_2$CH$_2$SH).

Preparation of Modified Silver Nanocrystals

Ag-(**1**+**2**) nanoparticles were prepared as already reported[18], using a solution of capping agents at a 9:1 molar ratio of **1** and **2**. The nanocrystals formed were precipitated by addition of ethanol, filtered off and washed with ethanol to obtain a dry gray powder redispersible in chloroform. The modified nanoparticles were used without any further purification. Transmission electron micrographs (TEMs) were obtained using a Philips CM 100 transmission electron microscope (Fig. 1).

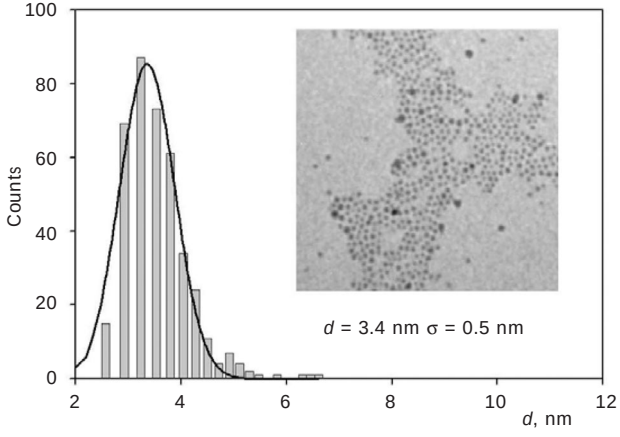

FIG. 1
Particle size histograms of as-produced silver nanoparticles by statistical analysis. Inset: transmission electron microscopy micrograph of as-prepared silver nanoparticles. For TEM investigations, a drop of nanoparticle solution in CH_2Cl_2 was transferred onto holey carbon foils supported on conventional copper microgrids. A Philips CM 100 transmission electron microscope, operating at 80 kV, was used

Electrode Modification

The electrodes used for nanoparticle immobilisation were 200 nm thick gold films evaporated in high vacuum on conductive fluorine-doped SnO_2 glass (sheet resistance of 8–10 Ω cm^{-2}). After immersion in a dilute solution of silver colloid in dichloromethane, the modified gold electrode was thoroughly rinsed with dichloromethane and dried before use.

Electrochemical Instrumentation and Measurements

Electrochemical experiments were performed in 1×10^{-1} M Na_2SO_4 aqueous solutions (pH 6.5), using a two-compartment electrochemical cell equipped with a saturated calomel electrode (SCE) and a platinum spiral as counter electrode. Cyclic voltammetric (CV), chronoamperometric and electrochemical impedance spectroscopy (EIS) experiments were carried out with an Autolab Model PGSTAT 30.

RESULTS AND DISCUSSION

Cyclic Voltammetry

The redox properties of the silver nanoparticle-modified gold electrodes were investigated by cyclic voltammetry and chronoamperometric experiments, which also allowed to estimate the surface coverage of the silver colloid. After modification, the gold electrode was transferred into the two-compartment electrochemical cell, containing an aqueous 1×10^{-1} M Na_2SO_4 solution. Figure 2a shows the CV curve obtained by performing repetitive potential scans under the above conditions. The first scan, from negative to positive potentials, displays a very broad oxidation peak in the region centred at 0.48 V, labelled as A′, and in the reverse scan a much narrower reduction peak at 0.10 V, labelled as B′. In the second scan, the height of the broad anodic peak is greatly diminished while a narrow peak appears at 0.22 V (A) whose height increases progressively in the following scans. At the same time, a new cathodic peak (B) increases at 0.07 V at the expense of that at 0.10 V. A similar behaviour was also found in aqueous $LiClO_4$ solutions.

The presence of isopotential points in the CV curves (at 0.09 and 0.24 V), associated with the conversion between two electroactive systems showing slightly different redox properties[19], would suggest that, during the first few potential scans, a significant reorganisation takes place in the silver colloid layer. Such a conversion would occur on the voltammetric time scale without any loss of electroactive material, as the overall charge underneath the two either anodic (A, A′) or cathodic (B, B′) peaks remains constant. The limiting CV pattern, obtained after *ca* ten scans, is shown in Fig. 2b: the peak morphology is that typical of redox processes involving surface-

confined species[20]. As expected for such a system, the peaks height was found to increase linearly with scan rate[20]. Furthermore, integration of the CV curve showed that, at any scan rate from 0.01 to 0.5 V s^{-1}, nearly the same charge is exchanged in the anodic and cathodic peaks (55.4 *vs* 55.0 μC cm^{-2}, respectively), as also confirmed by chronoamperometric experiments. The two peaks in Fig. 2b are therefore coupled to each other as partners of a reversible redox couple confined at the surface of the gold electrode. In agreement with such a hypothesis, Fig. 3 shows that reduction process B is only observed when the electrode first undergoes the oxidation process A, and *vice versa*. It also indicates that, on the time scale of the CV experiment, both processes are quantitative.

Such a reversible redox process is clearly associated with the presence of the silver colloid on the gold surface. Under the employed experimental conditions, in fact, the unmodified gold electrode only displays a purely capacitive behaviour, characterised by a much larger capacitive current than in the modified electrode (dashed line in Fig. 2b). The low double-layer capacitance observed in the latter case, on the other hand, is typical of electrodes carrying self-assembled monolayers (SAM) of long-chain thiols[21]. The CV response of the gold substrate supporting a SAM of dodecanethiols is compared in Fig. 2b (dot-and-dash) with the preceding ones, displaying in fact a greatly diminished capacitive current comparable to that of nano-

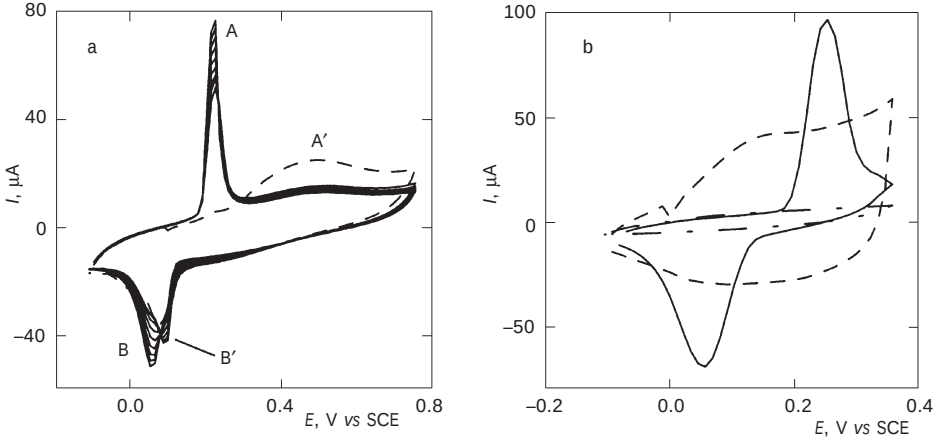

FIG. 2

a Consecutive cyclic voltammetric curves of as-prepared Ag colloid film on Au electrode in an aqueous 1×10^{-1} M Na_2SO_4 solution. The dashed line corresponds to the first scan; b full line: as in a after *ca* ten scans, dashed line: clean Au surface, dot-and-dashed line: Au modified by a dodecanethiol SAM. Scan rate: 0.05 V s^{-1}, T = 25 °C

particle-modified electrodes. The oxidation and reduction peaks in Figs 2 and 3 are therefore attributed to a process involving silver nanoparticles and, in particular, to the formation of a silver oxide or hydroxide layer over the colloid surface, during the positive scan, and to the corresponding reductive stripping, during the reverse scan. At the operating pH, the formation of an (hydr)oxide silver layer is in fact thermodynamically allowed at potentials higher than 0.1 V (*vs* SCE)[22]. Such a hypothesis was confirmed by comparison with a massive silver electrode modified with a SAM of dodecanethiols, displaying a very similar CV behaviour. Furthermore, a similar CV behaviour, also attributed to the formation of a densely packed monolayer of hydroxide species, has been reported for colloidal gold nanoparticles confined on ITO *via* an (aminopropyl)siloxane film[13,14].

In order to estimate the surface density of silver nanoparticles on the gold electrode surface, the charge exchanged at the CV peaks (Fig. 2) was considered. By combining such a value with (i) the monolayer capacity of silver (280 μC cm^{-2})[23], (ii) the diameter of silver particles as obtained by the TEM measurements, and (iii) assuming that the entire surface of each nanoparticle undergoes the redox process, the surface density of the self-assembled colloid monolayer was estimated to be 9.7×10^{10} particle cm^{-2}. Such a low value would correspond to a rather loose packing of the silver nanoparticles on the gold surface, the upper limit, corresponding to the dense packing as shown from the TEM image, being 4×10^{12} particle cm^{-2}.

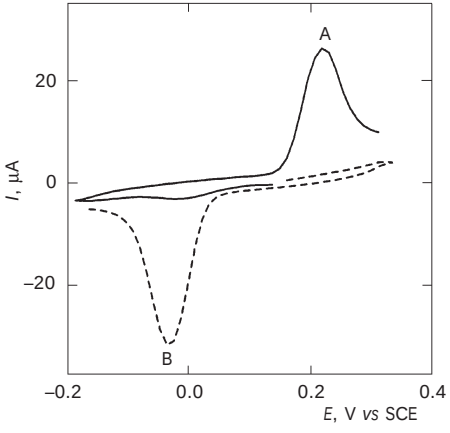

FIG. 3

Two consecutive CV curves of Ag colloid film onto Au electrode in an aqueous 1×10^{-1} M Na_2SO_4 solution, after initial conditioning as shown in Fig. 2a. Potential sequences: first scan (full line) +0.15/–0.18/+0.3 V, second scan (dashed line) +0.15/+0.3/–0.18 V. Scan rate: 0.1 V s^{-1}, T = 25 °C

The CV experiments would therefore indicate that only 5% of the gold surface is covered. However, the very low capacitive current measured at the modified electrodes, and the results of the electrochemical impedance spectroscopic investigation (*vide infra*), suggest that such a coverage is underestimated, likely due to the fact that the silver surface actually involved in the redox process is only a fraction of the whole nanoparticle surface. This would not be surprising in view of the well-known highly blocking properties of SAMs of long-chain thiols on coin metals (*vide infra*)[21].

Electrochemical Impedance Spectroscopy

EIS investigation of the modified electrode/solution interface was carried out under the same conditions used in the CV and chronoamperometric experiments, since EIS allows a much closer inspection of the electrical structure of the interface with respect to capacity measurements based on CV or chronoamperometry[24]. EIS has been largely used for investigating the kinetics of redox processes occurring at *n*-alkanethiol-coated electrodes[21–25], and was also used to study the electrochemical properties of metal nanoparticle colloids, either in solution or immobilised on conductive supports[15,16]. In EIS, the current is measured under potentiostatic control, *i.e.*

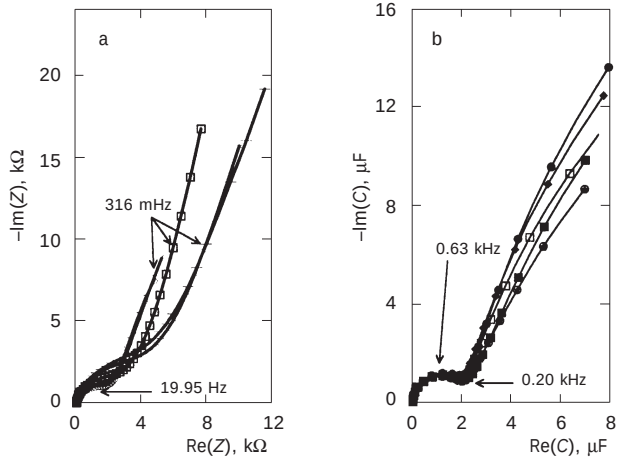

FIG. 4

Complex plane plots of the impedance (a) and complex capacitance (b) of Ag colloid film on Au electrode in an aqueous 1×10^{-1} M Na_2SO_4 solution, after initial conditioning as shown in Fig. 2a. The frequency range was 0.1 Hz–100 kHz. Applied potentials (in V): –0.30 (●), –0.05 (▲), 0.20 (□), 0.45 (■), 0.70 (Δ)

at a constant bias, while a small-amplitude sinusoidal voltage signal is applied to the electrochemical cell[24]. Excitation frequencies (f) between 1 mHz and 1 MHz can be used, thereby permitting in principle the investigation of phenomena on time scales ranging over 9 decades, which may be resolved in the EIS spectra according to their relaxation time. In Fig. 4, the impedance data recorded at various biases, from negative (–0.3 V) to positive values (+0.7 V), *i.e.* across the region where oxidation of nanoparticles occurs, are shown.

Two alternative presentations of the data sets were used. In Fig. 4a, the out-of-phase component of the impedance, –Im(Z), is plotted *vs* the in-phase one, Re(Z), –Im(Z) and Re(Z) being parametric functions of the frequency (z-plot or Nyquist plot)[20b,24]. Such a presentation emphasises the interface response at relatively low frequencies. In Fig. 4b, the complex capacitance C is plotted (c-plot), where $C = 1/j\omega Z$, $j = \sqrt{-1}$ and ω the angular frequency ($= 2\pi f$)[27]. The c-plot emphasises the interface response at higher frequencies with respect to the z-plot[25e,26]. The electrical response of the (modified) electrode/electrolyte interface at various frequencies of the sinusoidal perturbation is usually described in terms of equivalent circuits[20b,24], such as that shown in Scheme 1, which reproduces the behaviour of the present system.

The EIS data shown in Fig. 4b evidence the blocking (capacitive) behaviour (series RC arrangement) characterising the interface at high ($f > 100$ Hz) frequency. The response at low frequency (Fig. 4a) reflects, instead, a poorly defined structure whose electrical behaviour is represented in the equivalent circuit of Scheme 1 by resistance R_x and capacitance C_x. The R and C elements in the equivalent circuit of Scheme 1 were evaluated by fitting procedures, using the CNLS method described by Boukamp[28]. In the circuit of Scheme 1, R_Ω represents the solution resistance, C_{dl} the double layer capacitance, while R_x and C_x are elements responsible for the interface behaviour at $f < 1$ Hz [29]. The best-fit values of the various elements in the circuit of Scheme 1 are reported as a function of potential in Table I.

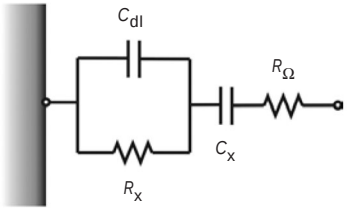

SCHEME 1

As expected, the value of R_Ω (the solution resistance) is essentially constant at the various potentials since such an element is not related to electrochemical processes occurring at the interface. Also C_{dl} was found to be almost invariant with potential. By contrast, R_x changes with potential. However, its value at 0.7 V is only twice as high as that at –0.3 V; such an element cannot therefore be associated to a faradaic process occurring at the interface. The observed dependence of both R_x and C_x on potential is possibly a consequence of the oxide-layer formation on the nanoparticle surface.

The low value for double layer capacitance C_{dl} is in agreement with the low capacitive currents measured by CV and is compatible with the presence of a rather compact organic layer on the gold electrode. In the case of a gold substrate modified with a SAM of dodecanethiol, the corresponding value was in fact *ca* 3.0 μF cm^{-2}. The very similar C_{dl} values obtained for the two systems would therefore suggest that the monolayer-coated silver

TABLE I
Calculated parameters from computer fitting (normalised to the electrode geometric area), using the equivalent circuit in Scheme 1 for the Ag colloid film on Au in an aqueous 1 × 10^{-1} M Na_2SO_4 solution (T = 25 °C)

E, V	R_Ω, Ω cm^2	C_{dl}, μF cm^{-2}	R_x, kΩ cm^2	$Y_0 \times 10^6$, Ω cm^2 s$^\varphi$ (φ)[a]
–0.30	88	3.3	1.50	1.6 (0.7)
–0.05	89	3.4	1.55	1.7 (0.7)
0.20	88	3.3	2.09	2.0 (0.7)
0.45	88	3.8	2.94	1.0 (0.7)
0.70	88	3.8	3.02	1.0 (0.7)

[a] See note[29].

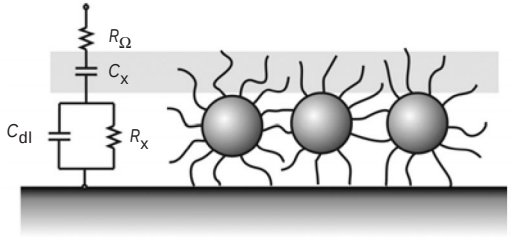

FIG. 5
Schematic representation and corresponding equivalent circuit of self-assembly of surface-active monolayer-coated Ag nanoparticles on Au electrode

nanoparticles are able to form a very compact film on the gold electrode, at variance with the low coverage value estimated from the CV charging experiments.

The structure of the silver nanoparticles film, as emerging from the analysis of the EIS data, characterised by a compact inner layer (having low capacitance) and a disordered outer one, may in principle explain the low charges associated with the oxide-layer formation, as deduced from the CV and chronoamperometric experiments. The oxidation process would in fact involve principally the fraction (<<1) of the nanoparticle surface that faces the aqueous solution and is free of thiols, being therefore in direct contact with the electrolyte (Fig. 5). Finally, the occurrence of the large-amplitude faradaic processes associated with the anodic growth/cathodic dissolution of silver oxide on/from the nanoparticle surface, and the relatively large double-layer capacitance displayed by the nanoparticle film, would explain why quantised capacitance charging phenomena[15,16] are not observed in the present system.

CONCLUSIONS

Self-assembling of monolayer-protected silver nanoparticles onto a gold electrode was obtained by using dithiol linkers. The nanoparticles were electrochemically surface-active, undergoing, in aqueous electrolyte, a reversible anodic oxidation process. Remarkably, the assembly remains stable over repetitive oxidation/reduction of the nanoparticle surface. Electrochemical impedance spectroscopy was used in order to characterise the electrochemical interface: all the impedance spectra, obtained at various potentials in the region of surface electroactivity of nanoparticles, were simulated by a relatively simple equivalent circuit in which two different capacitive elements account for the response, at high and low frequency, of the interface. Such elements were associated, respectively, to an inner and compact alkanethiol layer interposed between the gold surface and the nanoparticles, and an outer and relatively looser alkanethiol layer located outside. The latter layer would allow easy permeation of electrolyte to large fractions of the silver surface thus explaining the observed CV behaviour.

This work was carried out with partial support by the University of Bologna ("Funds for Selected Research Topics"), MIUR (PRIN 2002, prot. 2002035735), and C.N.R. (Agenzia 2000). We would like to thank Dr G. Falini for his help in the TEM investigation.

REFERENCES AND NOTES

1. a) Ryan D., Rao S. N., Rensmo H., Fitzmaurice D., Preece J. A., Wenger S., Stoddart J. F., Zaccheroni N.: *J. Am. Chem. Soc.* **2000**, *122*, 6252; b) Herranz M. A., Colonna B., Echegoyen L.: *Proc. Natl. Acad. Sci. U.S.A.* **2002**, *99*, 5040.
2. Venturi M., Credi A., Balzani V.: *Molecular Devices and Machines – A Journey into the Nanoworld*. Wiley-VCH, Weinheim 2003.
3. Wolfbeis O. S.: *Anal. Chem.* **2000**, *72*, 81.
4. Maxwell D. J., Taylor J. R., Nie S.: *J. Am. Chem. Soc.* **2002**, *124*, 9606.
5. Mayor M., Buschel M., Fromm K. M., Lehn J. M., Daub J.: *Chem. Eur. J.* **2001**, *7*, 1266.
6. Cavallini M., Biscarini F., Léon S., Zerbetto F., Bottari G., Leigh D. A.: *Science* **2003**, *299*, 531.
7. Sun S., Chong K. S. L., Leggett G.: *J. Am. Chem. Soc.* **2002**, *124*, 2414.
8. a) Rao C. N. R., Kulkarni G. U., Thomas P. J., Edwards P. P.: *Chem. Soc. Rev.* **2000**, *29*, 27; b) Mikrajuddin, Shi F. G., Nieh T. G., Okuyama K.: *Microelectronics J.* **2000**, *31*, 343; c) Xia Y., Gates B., Yin Y., Lu Y.: *Adv. Mater.* **2000**, *12*, 693.
9. Montalti M., Prodi L., Zaccheroni N., Falini G.: *J. Am. Chem. Soc.* **2002**, *124*, 13540.
10. Watanabe S., Sonobe M., Arai M., Tazume Y., Matsuo T., Nakamura T., Yoshida K.: *Chem. Commun.* **2002**, 2866.
11. Zamborini F. P., Leopold M. C., Hicks J. F., Kulesza P. J., Malik M. A., Murray R. W.: *J. Am. Chem. Soc.* **2002**, *124*, 8958.
12. a) Brust M., Bethell D., Schiffrin D. J., Kiely C. J.: *Adv. Mater.* **1995**, *7*, 795; b) Harfenist S. A., Wang Z. I., Alvarez M. M., Vezmar I., Whetten R. L.: *J. Phys. Chem.* **1996**, *100*, 13904; c) Sarathy K. V., Raina G., Yadav R. T., Kulkarni G. U., Rao C. N. R.: *J. Phys. Chem. B* **1997**, *101*, 9876; d) Musick M. D., Keating C. D., Keefe M. H., Natan M. J.: *Chem. Mater.* **1997**, *9*, 1499; e) Blonder R., Sheeney L., Willner I.: *Chem. Commun.* **1998**, 1393; f) Brust M., Bethell D., Kiely C. J., Schiffrin D. J.: *Langmuir* **1998**, *14*, 5425; g) Zhu T., Zhang X., Wang J., Fu X., Liu Z.: *Thin Solid Films* **1998**, *327–329*, 595; h) Gittins D. I., Bethell D., Nichols R. J., Schiffrin D. J.: *Adv. Mater.* **1999**, *11*, 737; i) Patolsky F., Ranjit K. T., Lichtenstein A., Willner I.: *Chem. Commun.* **2000**, 1025; j) Chen S., Huang K.: *J. Cluster Sci.* **2000**, *11*, 405; k) Shipway A. N., Willner I.: *Chem. Commun.* **2001**, 2035; l) Mandal S., Gole A., Lala N., Gonnade R., Ganvir V., Sastry M.: *Langmuir* **2001**, *17*, 6262; and references[6–8] therein; m) Manna A., Imae T., Iida M., Hisamatsu N.: *Langmuir* **2001**, *17*, 6000.
13. a) Brust M., Kiely C.: *Colloids Surf., A* **2002**, *202*, 175; b) Saraty K. V., Yhomas P. J., Kulkarni G. U., Rao C. N. R.: *J. Phys. Chem. B* **1999**, *103*, 399; c) Lahav M., Shipway A. N., Willner I.: *J. Chem. Soc., Perkin Trans. 2* **1999**, 1925.
14. Shipway A. N., Katz E., Willner I.: *ChemPhysChem.* **2000**, *1*, 18.
15. a) Snow A. W., Ancona M. G., Kruppa W., Jernigan G. G., Foos E. E., Park D.: *J. Mater. Chem.* **2002**, *12*, 1222; b) Chen S., Pei R., Zhao T., Dyer D. J.: *J. Phys. Chem. B* **2002**, *106*, 1903; c) Chen S.: *J. Phys. Chem. B* **2000**, *104*, 663; d) Chen S., Murray R. W.: *J. Phys. Chem. B* **1999**, *103*, 9996; e) Chen S., Ingram R. S., Hostetler M. J., Pietron J. J., Murray R. W., Schaaf T. G., Khoury J. T., Alvarez M. M., Whetten R. L.: *Science* **1998**, *280*, 2098.
16. a) Hicks J. F., Templeton A. C., Chen S., Sheran K. M., Jasti R., Murray R. W., Debord J., Schaaf T. G., Whetten R. L.: *Anal. Chem.* **1999**, *71*, 3703; b) Chen S., Sommers J. M.: *J. Phys. Chem. B* **2001**, *105*, 8816; c) Chen S., Murray R. W., Feldberg S. W.: *J. Phys. Chem. B* **1998**, *102*, 9898.

17. Fan F. F., Bard A. J.: *J. Phys. Chem. B* **2002**, *106*, 279.
18. Fullam S., Nagaraja Rao S., Fitzmaurice D.: *J. Phys. Chem. B* **2000**, *104*, 6164.
19. a) Paolucci F., Marcaccio M., Paradisi C., Roffia S., Bignozzi C. A., Amatore C.: *J. Phys. Chem. B* **1998**, *102*, 4759; b) Kuchynka D. J., Kochi J. K.: *Inorg. Chem.* **1988**, *27*, 2574; and reference[42] therein.
20. a) Bockris J. O'M., Khan S. U.: *Surface Electrochemistry, A Molecular Level Approach*, Chap. 7. Plenum, New York 1993; b) Bard A. J., Faulkner L. R.: *Electrochemical Methods*, 2nd ed. Wiley, New York 2001.
21. Finklea H. O. in: *Electroanalytical Chemistry* (A. J. Bard, Ed.), Vol. 19, p. 109. Marcel Dekker, New York 1996.
22. Vanleugenhaghe C., Pourbaix M., Van Rysselberghe P. in: *Atlas of Electrochemical Equilibria in Aqueous Solutions* (M. Pourbaix, Ed.), p. 393. Pergamon, Oxford 1966.
23. Vashkyalis A., Demontaite O.: *Elektrokhimiya* **1978**, *14*, 1213.
24. MacDonald J. R.: *Impedance Spectroscopy; Emphasizing Solid Materials and Systems*. Wiley, New York 1987.
25. a) Protsailo L. V., Fawcett W. R.: *Electrochim. Acta* **2000**, *45*, 3497; b) Dijksma M., Boukamp B. A., Kamp B., van Bennekom W. P.: *Langmuir* **2002**, *18*, 3105; c) Cui X., Jiang D., Diao P., Li J., Tong R., Wang X.: *J. Electroanal. Chem.* **1999**, *470*, 9; d) Flink S., van Veggel F. C. J. M., Reinhoudt D. N.: *Adv. Mater.* **2000**, *12*, 1315; e) Gafni Y., Weizman H., Libman J., Shanzer A., Rubinstein I.: *Chem. Eur. J.* **1996**, *2*, 759; f) Janek R. P., Fawcett W. R., Ulman A.: *J. Phys. Chem. B* **1997**, *101*, 8550.
26. Rubinstein I., Sabatani E., Rishpon J.: *J. Electrochem. Soc.* **1987**, *134*, 3078.
27. Note that, in the frame of an equivalent circuit description of the electrochemical interface, a semicircle in the *z*-plot corresponds to RC (resistor, capacitor) elements in parallel and a straight vertical line to RC elements in series, and *vice versa* in the case of *c*-plot[20b,25e,26].
28. Boukamp B. A.: *Solid State Ionics* **1986**, *20*, 31.
29. Because of the <90° slope of the low-frequency straight line in Fig. 4a, the capacitance C_x was treated as a (capacitive) constant phase element (CPE) for which impedance is given by $Z_Q = 1/[Y_0(j\omega)^{\varphi}]$, where Y_0 is a proportionality constant and φ is an exponent between 0 and 1. For $\varphi = 1$, Y_0 is a pure capacitance. The use of CPE is a common procedure in the presence of non-ideal behaviour in the impedance spectra, such as <90° slopes and depressed semicircles[25b,25e]. Although there is no general agreement on the interpretation of CPE in electrochemical systems, such non-idealities have often been associated with anomalous transport effects in porous film electrodes: a) Bisquert J., Garcia-Belmonte G., Fabregat-Santiago F., Compte A.: *Electrochem. Commun.* **1999**, *1*, 429; b) Zoltowski P.: *J. Electroanal. Chem.* **1998**, *443*, 149; c) Láng G., Heusler K. E.: *J. Electroanal. Chem.* **1998**, *457*, 257; d) Sadkowski A.: *J. Electroanal. Chem.* **2000**, *481*, 222.